

COMBINING QUADRUPOLE-DRIVEN SLOW EXTRACTION WITH RFKO AT THE CERN SPS

P. A. Arrutia Sota *, M. A. Fraser, T. Levens, F. M. Velotti, CERN, Switzerland

Abstract

The CERN Super Proton Synchrotron (SPS) employs quadrupole-driven third-integer slow extraction to deliver beam to the North Area. This process is controlled by ramping all the magnets in the lattice, gradually driving the circulating beam into the tune resonance. In medical synchrotrons, Radio-Frequency Knock Out (RFKO) has proven to be a reliable alternative for driving the extraction process while maintaining good spill quality. Inspired by these efforts, a hybrid scheme was tested in the SPS, where a transverse exciter was used to apply a sinusoidal excitation in parallel with the magnetic ramp. It is demonstrated that this setup improves spill uniformity both in simulation and measurements.

INTRODUCTION

The North Area users at CERN receive proton beams from the SPS at 400 GeV/c. The beam is extracted via third-integer resonant slow extraction by setting the machine's horizontal tune at $Q = \frac{80}{3}$ and slowly driving the de-bunched beam of particles into resonant motion. To achieve this, all magnets in the ring are ramped together, which effectively results in a changing momentum offset $\Delta p/p_0$ that modifies the beam's tune through chromaticity [1]. Such a method delivers a flux of particles $n(t)$ over several seconds, whose quality can be quantified by analysing the magnitude a_f of the modulations at a given frequency f :

$$a_f = \left| \frac{\int_0^T n(t) e^{2\pi i f t} dt}{\int_0^T n(t) dt} \right|, \quad (1)$$

where T is the duration of the spill.

In the SPS, the slow (Hz-kHz) spill modulations are dominated by the 50 Hz component $a_{50\text{Hz}}$, which stems from the power-converter ripple remaining after AC-to-DC rectification of the main grid voltage. If left uncorrected, this can lead to unacceptable spill quality for the users and, ultimately, downtime and loss of valuable data. In recent years, a variety of techniques have been deployed in the SPS to counteract this effect [2, 3]. Still, R&D on this topic remains an active subject of investigation, searching for more effective and maintainable solutions.

RFKO IN THE SPS

The Radio-Frequency (RF) technique known as empty-bucket channelling has proven extremely useful in the SPS for suppressing spill ripple [2]. In such an approach, the momentum ramp is supplemented with longitudinal kicks

from an RF cavity to help the beam cross the tune-resonance boundary. In this contribution, we use a similar principle but instead apply transverse kicks with an RF exciter. In other words, in addition to the $\Delta p/p_0$ change from the magnetic ramp, each particle i receives a turn-by-turn horizontal kick $\Delta x'_i$,

$$\Delta x'_i = k \sin(2\pi q_{\text{exc}} f_0 \tau_i + \phi), \quad (2)$$

where f_0 is the revolution frequency, τ_i is the particle's time of arrival, and k , q_{exc} , ϕ are the exciter gain, tune and phase, respectively.

The scheme is inspired by the RF Knock-Out (RFKO) method used in many medical facilities [4, 5], where the exciter is employed as the only mechanism to drive the slow-extraction process. Studies have shown that such a method can be effective at suppressing spill ripple [6]. Here, however, both the ramp and the exciter are combined, as shown in Fig. 1. The exciter parameters k , q_{exc} , ϕ are kept fixed throughout the entire spill.

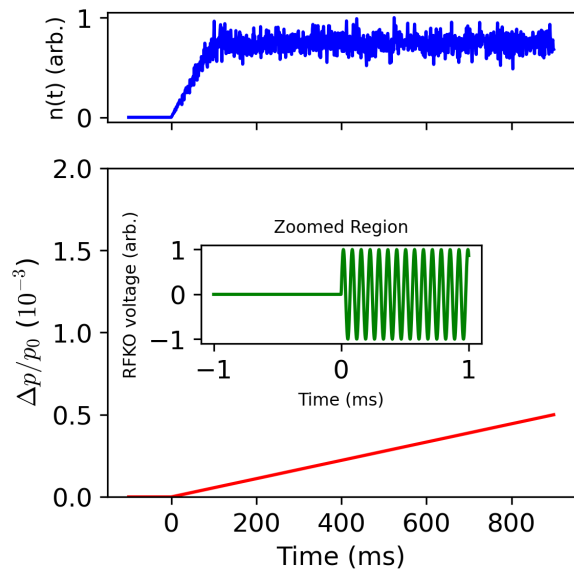


Figure 1: Sketch of the combined slow-extraction scheme in the SPS. The slow extraction starts at $t = 0$ by ramping the reference momentum and activating the RFKO transverse excitation, which together control the extracted particle flux $n(t)$.

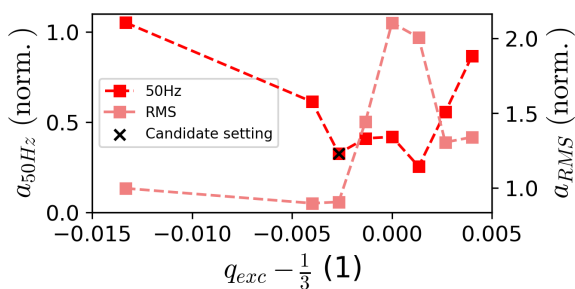
SPILL-QUALITY MEASUREMENTS

A measurement campaign was conducted in the SPS to measure the impact of the exciter on the spill quality. During the test, the exciter gain k was set to the maximum value allowed by the control system (arbitrary units), and the exciter tune was varied around the fundamental harmonic of

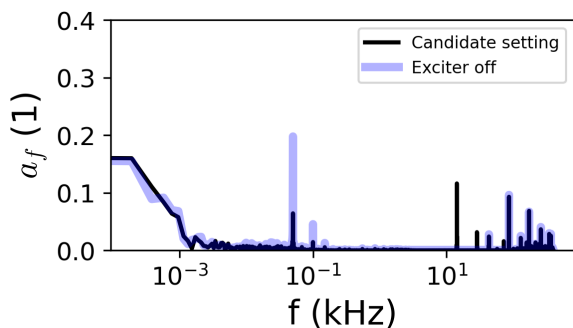
* pablo.arrutia@cern.ch

the third-integer resonance, i.e. $q \approx \frac{1}{3}$. The results of such a test are shown in Fig. 2. It can be seen that, when the exciter tune is correctly set, substantial reduction of the 50 Hz ripple can be observed. On the other hand, the exciter introduces spectral components at the excitation frequency and harmonics thereof at much higher frequencies. This appears as a degradation of the overall root-mean-squared (RMS) spectral amplitude a_{RMS} , measured up to 800 kHz.

A candidate setting has been selected for illustration purposes, which balances the low-frequency improvement and the high-frequency modulation, achieving an overall improvement in a_{RMS} of $\sim 10\%$. Further discussions are needed with experimental users to understand if such a setup is ultimately beneficial, or whether one would have to operate the exciter at a higher harmonic to ‘hide’ the modulation beyond the users’ acquisition bandwidth.



(a) 50Hz and RMS spectral amplitudes $a_{50\text{Hz}}$ and a_{RMS} (up to 800 kHz) as a function of exciter tune q_{exc} , normalised to scenario where exciter is off.



(b) Entire a_f spectrum, exciter off vs. exciter on with optimised settings.

Figure 2: Measurements of the spill spectral components a_f for different exciter configurations.

MODEL FITTING WITH MACHINE LEARNING

It has been empirically demonstrated that the combined slow-extraction method described above can successfully suppress the 50 Hz spill ripple. However, it is useful to construct tracking simulations that reproduce the phenomenon, with the aim to further optimise the settings of the exciter as well as improve our understanding of the beam dynamics. To do so, we employ an *henon-like* map model of the SPS

slow extraction (see [7] for details), where the action of the transverse exciter has been implemented following Eq. (2). The goal is to fit the model’s parameters to reproduce as closely as possible the observed data behaviour from Fig. 2. In particular, we choose the chromaticity Q' , the resonance-driving term S and the exciter gain k (in number of beam sigmas) as our fitting parameters, as they all contribute significantly to the ripple suppression process [6, 8].

Fitting Procedure

Spill simulations via particle tracking are computationally expensive. For the SPS slow extraction, one often needs to simulate $\sim 10^5$ particles over $\sim 10^5$ turns to resolve the 50 Hz modulations in the extracted flux. Therefore, grid searches become extremely inefficient for multi-parameter fitting tasks. Instead, a more sample-efficient approach is adopted here. First, 500 samples are simulated via tracking, whose parameters (q, S, Q', k) have been pseudo-randomly selected using the Sobol’ sequence [9]. Then, the output $a_{50\text{Hz}}$ of such simulations is employed to train a neural network that estimates the mapping $(q, S, Q', k) \rightarrow a_{50\text{Hz}}$. This neural network will replace the tracking code during the fitting procedure, acting as a surrogate model capable of estimating $a_{50\text{Hz}}$ at a fraction of the computational cost. The workflow is illustrated in Fig. 3.

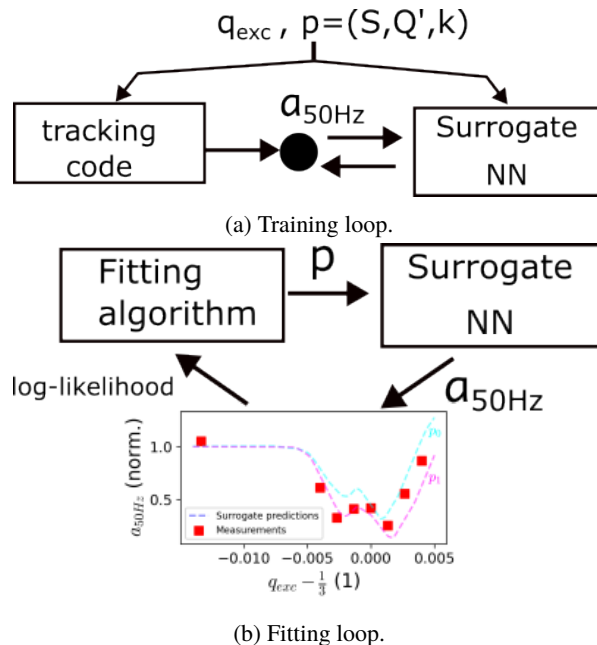


Figure 3: Training and fitting workflow employed to fit tracking simulations to measurement data. A neural network (NN) is used as a surrogate model of the tracking code.

For the fitting task, Markov Chain Monte Carlo (MCMC) was used. In the context of parameter fitting, MCMC allows us to infer posterior distributions over model parameters rather than single point estimates. MCMC collects chains of samples in the parameter space, whose distribution converges towards the equilibrium distribution that maximises

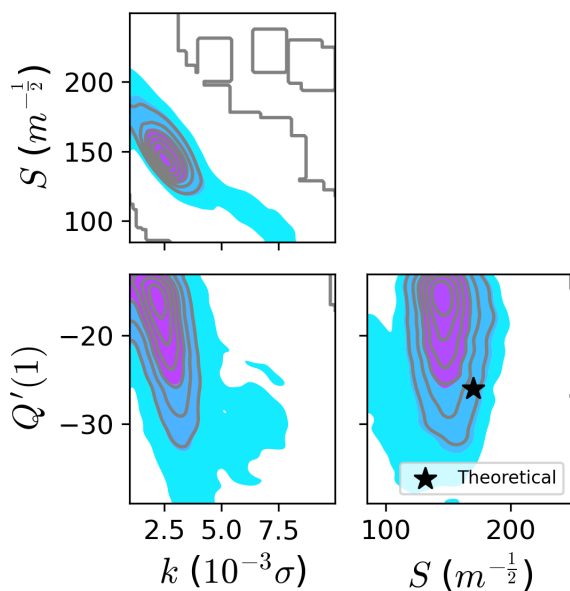


Figure 4: 2-D projections of the posterior distribution obtained via MCMC for the fitting parameters. The prior was initialised uniformly over the shown parameter space. The star shows the theoretical chromaticity Q' and resonance-driving term S for the SPS fixed-target working point.

the log-likelihood of observing the measurement data. The approach remains robust even in under-constrained situations and does not assume that the estimate uncertainties are normally distributed. MCMC requires a large amount of samples to converge, but our surrogate model now allows us to exploit it at practically no computational cost.

Results

The posterior distribution obtained via MCMC is shown in Fig. 4. The best fit is given by the parameter set that maximises the likelihood, $S = 146 m^{1/2}$, $Q' = -22$, $k = 0.003 \sigma$. Interestingly, the fitted S and Q' values are somewhat different from the theoretical working point ($S = 170 m^{1/2}$, $Q' = -26$), although the latter still falls well within the uncertainty of the fit. The discrepancy may also stem from the simplicity of the *henon-like* tracking model.

Figure 5 displays the dependence of $a_{50\text{Hz}}$ on the exciter tune q for the measurement data, the surrogate model and the tracking simulations. The tracking simulations have been executed using the best fit parameters only, while the surrogate model predictions include the 10-90% inter-quantile range, after analysing the output of 1000 parameter combinations sampled from the posterior in Fig. 4. It can be seen that both the surrogate model and the tracking simulations agree very well with the measurement data. It must be emphasised that the tracking results were only used during training, but never during fitting. Thus, the strong agreement between the tracking and the measurements suggests that the surrogate model correctly learned the underlying dynamics of the simulation.

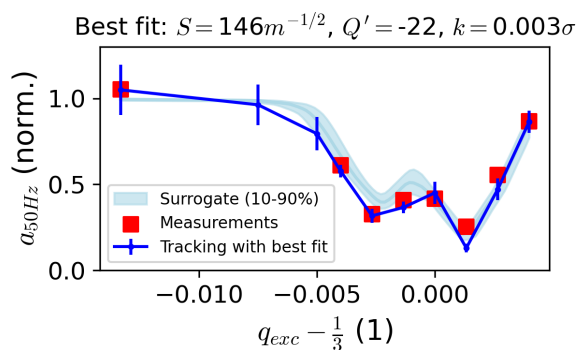


Figure 5: 50Hz ripple amplitude $a_{50\text{Hz}}$ vs. exciter tune q for measurement data, fitted surrogate model and tracking simulation employing best-fit parameters.

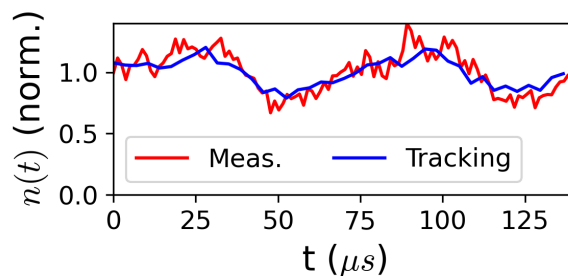


Figure 6: Spill structure at the exciter timescale (measured and simulated) for the candidate configuration from Fig. 2. Only two exciter periods are shown, but the structure repeats throughout the whole spill.

HIGH-FREQUENCY STRUCTURE

The fitted tracking model can now be exploited for additional studies. As an example, Fig. 6 shows the high-frequency structure introduced by the exciter for the candidate setting configuration from Fig. 2. Excellent agreement can be observed between the measurement and the tracking. This further validates the model and opens up the possibility to use it offline for detailed optimisation studies.

CONCLUSION

This work introduced a new slow-extraction scheme at the CERN SPS, combining the nominal magnetic ramp with a transverse sinusoidal excitation to suppress unwanted flux modulations. Additionally, a neural-network surrogate model was used to replace tracking simulations during fitting, enabling efficient posterior estimation with MCMC. Future efforts will focus on optimising exciter parameters and exploring a multi-fidelity approach.

ACKNOWLEDGMENTS

The authors would like to acknowledge M. Delrieux, who had already tried a practically identical slow-extraction technique in the CERN Proton Synchrotron.

REFERENCES

- [1] V. Kain *et al.*, “Resonant slow extraction with constant optics for improved separatrix control at the extraction septum”, *Phys. Rev. Accel. Beams*, vol. 22, no. 10, p. 101 001, 2019. doi : 10.1103/PhysRevAccelBeams.22.101001
- [2] P. A. Arrutia Sota *et al.*, “Empty-bucket techniques for spill-quality improvement at the CERN Super Proton Synchrotron”, *Phys. Rev. Accel. Beams*, vol. 27, no. 7, p. 074 001, 2024. doi : 10.1103/PhysRevAccelBeams.27.074001
- [3] V. Kain *et al.*, “Slow extracted spill ripple control in the CERN SPS using adaptive Bayesian optimisation”, in *Proc. IPAC’24*, Nashville, TN, USA, pp. 1790–1793, 2024. doi : 10.18429/JACoW-IPAC2024-TUP55
- [4] K. Noda *et al.*, “Advanced RF-KO slow-extraction method for the reduction of spill ripple”, *Nucl. Instrum. Methods Phys. Res., Sect. A*, vol. 492, no. 1–2, pp. 253–263, 2002. doi : 10.1016/s0168-9002(02)01319-0
- [5] P. Meliga, E. Bressi, G. Debernardi, L. Falbo, and C. Priano, “Design and commissioning of the RF-KO extraction at CNAO”, in *Proc. IPAC’23*, Venice, Italy, pp. 162–164, 2023. doi : 10.18429/JACoW-IPAC2023-MOPA060
- [6] P. Niedermayer and R. Singh, “Excitation signal optimization for minimizing fluctuations in knock out slow extraction”, *Sci. Rep.*, vol. 14, p. 10 310, 2024. doi : 10.1038/s41598-024-60966-y
- [7] P. Arrutia, “Advanced RF techniques for CERN’s future slow-extracted beams”, Presented 06 Mar 2024, U. Oxford (main), 2024. <https://cds.cern.ch/record/2900716>
- [8] M. Pari, F. M. Velotti, M. A. Fraser, V. Kain, and O. Michels, “Characterization of the slow extraction frequency response”, *Phys. Rev. Accel. Beams*, vol. 24, no. 8, p. 083 501, 2021. doi : 10.1103/PhysRevAccelBeams.24.083501
- [9] I. M. Sobol’, “On the distribution of points in a cube and the approximate evaluation of integrals”, *USSR Computational Mathematics and Mathematical Physics*, vol. 7, no. 4, pp. 86–112, 1967. doi : 10.1016/0041-5553(67)90144-9